Proc. Natl. Acad. Sci. USA
Vol. 92, pp. 4882–4886, May 1995
Neurobiology

Structural conservation of ion conduction pathways in K channels and glutamate receptors

(membrane topology/*N*-methyl-D-aspartate receptors/glycosylation)

MICHAEL W. WOOD, HENDRIKA M. A. VANDONGEN, and ANTONIUS M. J. VANDONGEN*

Department of Pharmacology, Duke University Medical Center, P.O. Box 3813, Durham, NC 27710

Communicated by Dale Purves, Duke University Medical Center, Durham, NC, February 8, 1995 (received for review December 20, 1994)

ABSTRACT **Single channel recordings demonstrate that ion channels switch stochastically between an open and a closed pore conformation. In search of a structural explanation for this universal open/close behavior, we have uncovered a striking degree of amino acid homology across the pore-forming regions of voltage-gated K channels and glutamate receptors. This suggested that the pores of these otherwise unrelated classes of channels could be structurally conserved. Strong experimental evidence supports a hairpin structure for the pore-forming region of K channels. Consequently, we hypothesized the existence of a similar structure for the pore of glutamate receptors. In ligand-gated channels, the pore is formed by M2, the second of four putative transmembrane segments. A hairpin structure for M2 would affect the subsequent membrane topology, inverting the proposed orientation of the next segment, M3. We have tested this idea for the NR1 subunit of the *N*-methyl-D-aspartate receptor. Mutations that affected the glycosylation pattern of the NR1 subunit localize both extremes of the M3–M4 linker to the extracellular space. Whole cell currents and apparent agonist affinities were not affected by these mutations. Therefore it can be assumed that they represent the native transmembrane topology. The extracellular assignment of the M3–M4 linker challenged the current topology model by inverting M3. Taken together, the amino acid homology and the new topology suggest that the pore-forming M2 segment of glutamate receptors does not transverse the membrane but, rather, forms a hairpin structure, similar to that found in K channels.**

Ion channels are large integral membrane proteins that form ion-selective pores. An important functional determinant is their mechanism of activation, which defines the two major classes of channels (1). Voltage-gated channels are activated by a change in membrane potential, whereas ligand-gated channels are activated by binding of a neurotransmitter to a receptor domain. Analysis of single ion channel behavior using the patch clamp technique has revealed a common functional characteristic: following activation, channels switch stochastically between an open and a closed pore conformation (2). In fact, the kinetic behavior of different channel types may be so similar that they cannot be easily distinguished (Fig. 1*A*). Although alternate channel-forming motifs exist [e.g., gramicidin (4)], one simple interpretation of this universal binary open/close behavior is that the pore-forming regions are structurally conserved.

Ligand- and voltage-gated channels are composed of subunits or domains surrounding a central ion-conducting pore. Despite this common feature, other aspects of quaternary structure remain distinct (Fig. 1 *B–D*). Voltage-gated channels consist of four domains or subunits (5), while ligand-gated channels consist of five subunits (6–8). Subunits or domains of voltage-dependent channels consist of six putative α-helical transmembrane segments, S1–S6. The amino acid sequence linking S5 and S6 contains a highly conserved amphiphatic region (H5 or P region), which forms the narrow part of the pore, including the selectivity filter (9–13). The structural model for ligand-gated channels is based mainly on data obtained for the nicotinic acetylcholine (nACh) receptor (14). Hydrophobicity analysis originally predicted the signal peptide-containing amino terminus and the carboxyl terminus to be extracellular and the four putative α-helical transmembrane segments (M1–M4) to each span the lipid bilayer once. The long segment linking M3 and M4 has a cytoplasmic localization in this model.

Although the secondary structure is not known, the tertiary structure of the pore region of voltage-gated K channels is a reentrant loop or hairpin, since charybdotoxin binding is affected by mutations flanking the region, positioning both ends of the pore externally (15, 16). Site-directed mutagenesis has implicated M2 in a pore-forming role for many ligand-gated channels (17–19). The originally proposed transmembrane topology of M2 (14) has been supported by experimental evidence in the nACh receptors (20, 21). Thus, the pore of voltage-gated channels is thought to be lined by four hairpins, while the pore of ligand-gated channels seems to be lined by five α-helical transmembrane segments.

The ligand-gated channel topology model with four transmembrane segments has recently been challenged for the glutamate receptor family (Fig. 1*E*). A protein kinase C phosphorylation site was identified in the carboxyl terminus of the NR1 subunit (22). Also, an N-linked glycosylation site (23, 24) and a protein kinase A phosphorylation site were reported to exist within the M3–M4 linker of GluR6 (3). A historic model with an additional transmembrane region between M3 and M4 (25, 26) was revived in order to account for these observations (21, 27). Homology with bacterial periplasmic binding proteins (28) and subsequent mutagenesis studies (29) have raised the possibility that the region immediately following M3 may contribute to ligand binding. An even number of transmembrane segments would have to precede this region if it indeed were external. A similar conclusion was reached in a study using *in vitro* translation of a kainate binding protein (30). Deletion of M2 did not affect downstream glycosylation, suggesting that M2 does not transverse the membrane. However, since functionality was not demonstrated for these proteins, adverse effects of mutagenesis on membrane topology could not be evaluated. It must be emphasized that any study attempting to elucidate native topology must demonstrate uncompromised function, since lack of function could reflect improper folding (31).

To investigate the possibility of a common structural motif for the pores of voltage- and ligand-gated channels, we have aligned the amino acid sequences of the respective pore-forming regions. A significant degree of homology was found

The publication costs of this article were defrayed in part by page charge payment. This article must therefore be hereby marked "*advertisement*" in accordance with 18 U.S.C. §1734 solely to indicate this fact.

Abbreviations: NMDA, *N*-methyl-D-aspartate; nACh, nicotinic acetylcholine; GABA, γ-aminobutyric acid.

*To whom reprint requests should be addressed.

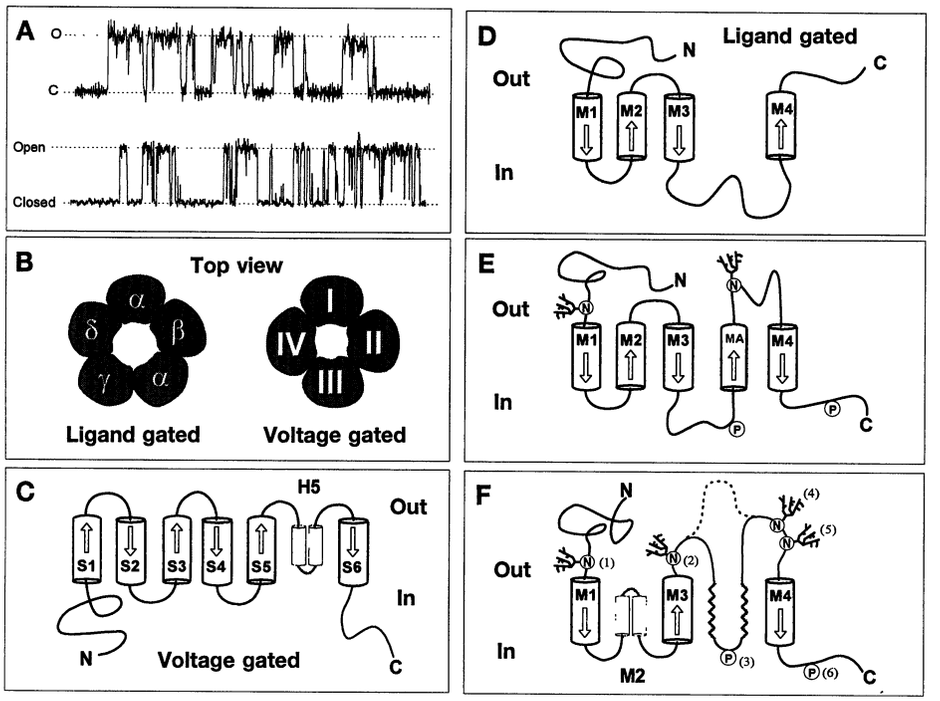

FIG. 1. Function and topology of voltage- and ligand-gated channels. (*A*) Patch clamp single channel records from a voltage-gated K channel (drk1) and a glutamate receptor [*N*-methyl-D-aspartate (NMDA) receptor NR1+NR2A], illustrating uniform, binary open/close behavior. (*B*) Voltage-gated channels consist of four domains or subunits; ligand-gated channels consist of five subunits. (*C*) Membrane topology of voltage-gated channels. Subunits or domains of voltage-dependent channels consist of six transmembrane segments (S1–S6). The pore region (H5) between S5 and S6 forms a hairpin. (*D*) Membrane topology of ligand-gated channels. The amino (N) and carboxyl (C) termini are extracellular and the four transmembrane domains (M1–M4) each span the lipid bilayer once. (*E*) Topology recently proposed for the glutamate receptors, taking into account two phosphorylation sites (P) and an N-linked glycosylation site (N). (*F*) Membrane topology for the NMDA receptor proposed in this paper including a hairpin pore structure (M2). It accounts for the inverted M3 orientation revealed by introduction of an N-glycosylation site (no. 2) immediately following M3. An N-glycosylation site (no. 1) present in GluR6, 16 residues upstream of M1, orients this segment (3). A functional phosphorylation site in GluR6 (no. 3) can be accommodated only by the introduction of two additional transmembrane segments. A phosphorylation site in NR1 (no. 6) as well as functional N-glycosylation sites in GluR6 (no. 4) and NR1 (no. 5) (this paper) are also indicated.

between K channels and glutamate receptors. If their pore structures were indeed conserved, then M2 would have to be a hairpin structure. The topological consequences of such an M2 pore structure were tested for the NR1 subunit of the NMDA receptor by altering the N-glycosylation pattern. The results obtained support the hairpin model for M2.

MATERIALS AND METHODS

Amino Acid Alignment. Amino acid sequences of the pore-forming regions of ligand- and voltage-gated channels were retrieved from GenBank and aligned as follows. The class of voltage-dependent channels contains three families, as defined by their ion selectivity: K^+, Na^+, and Ca^{2+} channels. The class of ligand-gated channels contains five families: nACh receptors, γ-aminobutyric acid type A (GABA) receptors, glycine receptors, glutamate receptors, and serotonin (5-hydroxytryptamine) 5HT3 receptors. First, amino acid sequences of intrafamily members were aligned, which was unambiguous due to the high degree of conservation. Then, families with known sequence homology were aligned. Four groups resulted: (*i*) GABA, glycine, nACh, and 5HT3 receptors, (*ii*) glutamate receptors, (*iii*) voltage-dependent K^+ channels, and (*iv*) voltage-dependent Na^+ and Ca^{2+} channels. Finally, these four groups were aligned with each other. The following conservative amino acid substitutions (single-letter code) were allowed: MILV (hydrophobic), EDRK (charged), FWY (aromatic), and AST (hydrophilic). Substitutions within a conserved group have coefficients >1.0 in the mutation matrix recommended for initially aligning proteins (32).

Western Analysis. Fifty to 80 *Xenopus laevis* oocytes were homogenized (33), followed by sucrose gradient centrifugation (34) to remove yolk protein. Membranes were solubilized (35) and subjected to either mock or endoglycosidase H (500 units each) treatment according to the manufacturer's protocol (New England Biolabs) with denaturing temperature reduced to 67°C. SDS/PAGE using 5% gels was performed, increasing the run time to enhance separation of proteins. Separated proteins were transferred electrophoretically to poly(vinylidene difluoride) membranes, incubated with a monoclonal NR1 antibody [54.1 Pharmingen (35)] followed by a secondary antibody conjugated to alkaline phosphatase (Sigma), and visualized by substrate detection (Bio-Rad).

Molecular Biology. Site-directed mutagenesis was performed using a megaprimer PCR method (36). Oligonucleotides were designed to engineer single amino acid substitutions into NR1. Mutations were confirmed by sequencing (United States Biochemical).

Electrophysiology. *X. laevis* oocytes were injected with 75 nl of cRNA (100 ng/μl) as described (37). Functional expression was assessed 2–5 days later using a two-electrode voltage-clamp amplifier (Warner Instruments, Hamden, CT) by application of agonists during continuous perfusion of 100 mM NaCl/5 mM KCl/2 mM $BaCl_2$/10 mM Hepes, pH 7.4, 25°C. Low-resistance glass electrodes (0.5–2 MΩ) were filled with 3 M KCl/10 mM Hepes, pH 7.4. Data acquisition and voltage control were accomplished with PCLAMP hardware and software (Axon Instruments, Burlingame, CA).

RESULTS AND DISCUSSION

Amino acid sequences of pore-forming regions of voltage- and ligand-gated channels were aligned and the main result is summarized in Fig. 2. The K^+ channel pore-forming regions

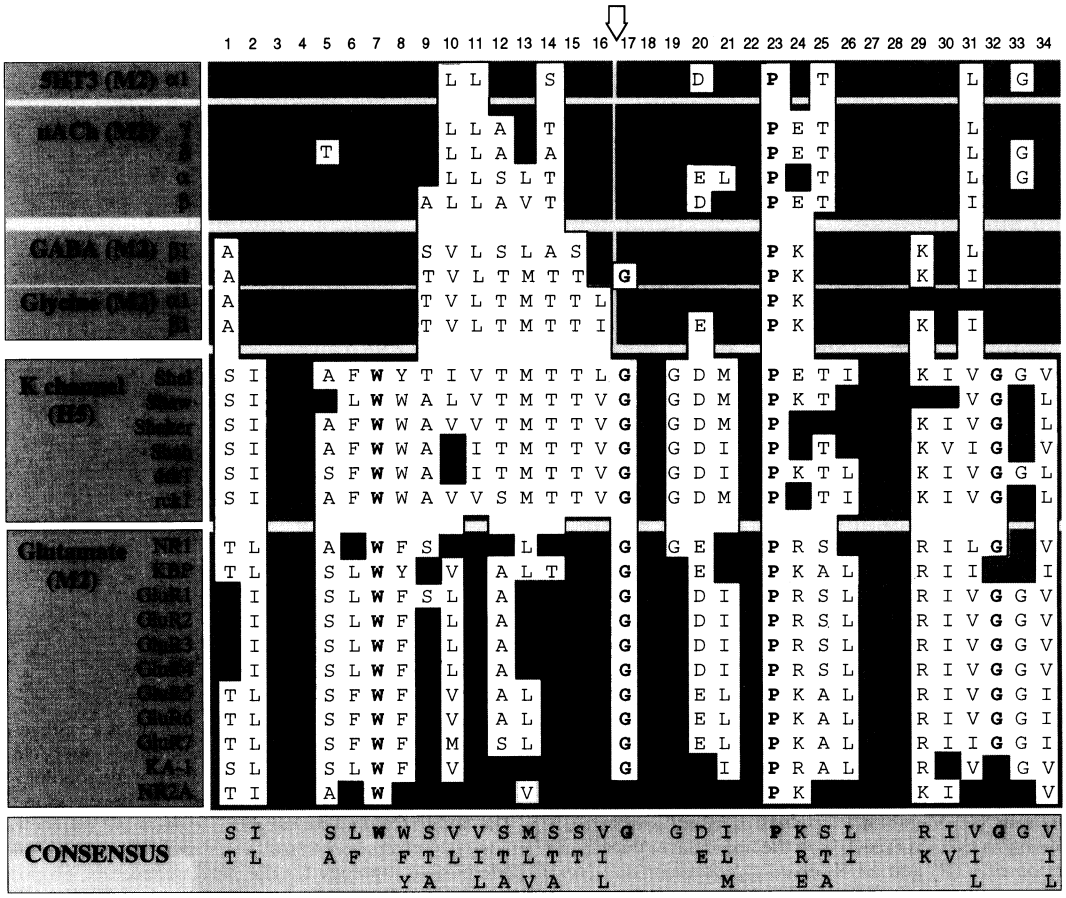

FIG. 2. Homology in pore regions of K channels and glutamate receptors. Amino acid sequences of pore regions were aligned as described in the text. Only limited homology was observed between the pore-forming regions of voltage-dependent K^+ channels and Na^+ and Ca^{2+} channels. Also, the glutamate receptors had no significant homology with the GABA–glycine–nACh–5HT group. Unexpectedly, however, the pore regions of K channels were found to have a large degree of homology with the pore regions of glutamate receptors. A much lesser degree of homology was observed between K channels and the remaining families of ligand-gated channels, which also required a 2-amino acid deletion between positions 16 and 17 (see arrow) in order to maintain the alignment. A consensus sequence was constructed containing amino acids that are conserved between the two classes of channels. Positions that contain an amino acid that belongs to the consensus sequences are shown on a white background; other positions have a dark background. Absolutely conserved residues are shown in boldface. The single-letter amino acid code is used.

showed a striking homology with the M2 segments of glutamate receptors. The homology extends over a region of 34 amino acids and includes the pore-forming regions (M2 and H5) as well as the first 4 or 5 amino acids of the following transmembrane segment (S6 and M3). The homology between the pore regions of the glutamate receptors and K channels is highly significant, with most members having 17–22 residues conserved from a total of 34. A notable exception is the NMDA receptor NR2 subunit, which has only 10 consensus residues. The other ligand-gated channels, including the acetylcholine, GABA, glycine, and serotonin 5HT3 receptors, show much weaker homology with K channels, with only 8–14 residues conserved. They also required a deletion of two amino acids (arrow in Fig. 2) in order to maintain the alignment. Nearly all ion channel sequences share a motif at the end of their pore-forming regions—a proline (P) followed by one of three charged residues: arginine (R), lysine (K), or glutamate (E).

The extended homology between the pore regions of voltage-gated K channels and glutamate receptors suggested that their structure could be conserved. The hairpin structure of the pore region of voltage-dependent K channels seems incontrovertible in light of cumulated experimental data. Structural conservation therefore implies a hairpin structure for M2, which would affect the orientation of the subsequent transmembrane segment (M3) since it adjoins M2 via a very short linker. In this case, the carboxyl terminus of M3 should be extracellular (Fig. 1*F*), not intracellular as in all current models (Fig. 1 *C–E*). We have tested this hypothesis for one member of the glutamate receptor family, the NR1 subunit of the NMDA receptor. Using site-directed mutagenesis, an N-linked glycosylation consensus sequence was introduced in the M3–M4 linker, 16 amino acids downstream of M3. Since 8 of these 16 residues are charged, the existence of an additional transmembrane segment can be ruled out. Western analysis demonstrated an increase in apparent molecular mass of this construct (P675A), confirming the addition of carbohydrate moieties to this sequence (Fig. 3*B*). Destruction of another glycosylation consensus sequence (S773A) 41 amino acids upstream of M4 resulted in a decrease in molecular mass, localizing the other extreme of the M3–M4 linker to the extracellular space. Digestion of proteins, isolated from wild-type and mutant NR1 injected oocytes, with endoglycosidase H removed all carbohydrate modifications and shifted the apparent molecular mass of all constructs back to the nonglycosylated form (Fig. 3*C*).

Both NR1 glycosylation mutants displayed normal whole-cell current responses when expressed in *X. laevis* oocytes (Fig. 4*A*). Dose–response curves for L-glutamate and glycine showed that the mutations did not affect the EC_{50} values for these two coagonists. Since the altered glycosylation pattern did not compromise function, we can assume that the topology of the NR1 subunit was not altered by these mutations. Interestingly, introduction of an additional glycosylation site

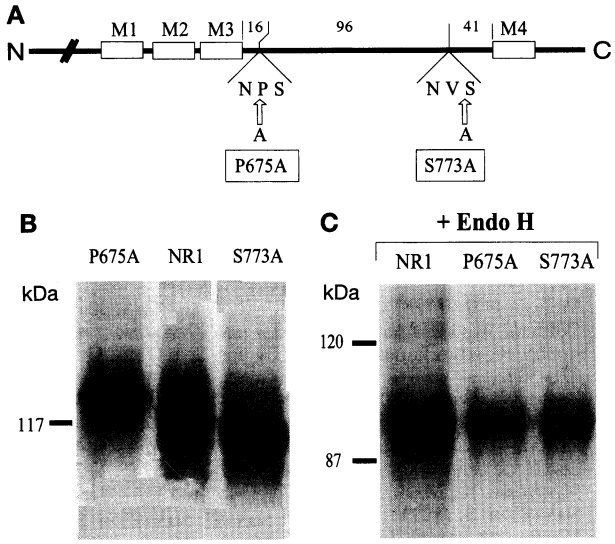

FIG. 3. Extracellular location of the M3–M4 linker inferred by alteration of N-glycosylation. (*A*) Site-directed mutagenesis (36) of the NR1 NMDA receptor subunit (a generous gift of Shigetada Nakanishi; ref. 38) was used to introduce an N-glycosylation consensus sequence (NxS, $x \neq$ P) 16 amino acids downstream of M3, by mutating proline 675 to alanine. Also, an existing consensus sequence (NVS) 41 amino acids upstream of M4 was destroyed by mutating serine 773 to alanine. (*B* and *C*) Western analysis was performed for NR1 and glycosylation mutants P675A and S773A expressed in *X. laevis* oocytes. Both mutants produced the predicted shifts in apparent molecular mass, confirming their extracellular location (37). These differences were due to altered carbohydrate modifications since digestion with endoglycosidase H reduced the molecular mass of all constructs to ≈97 kDa.

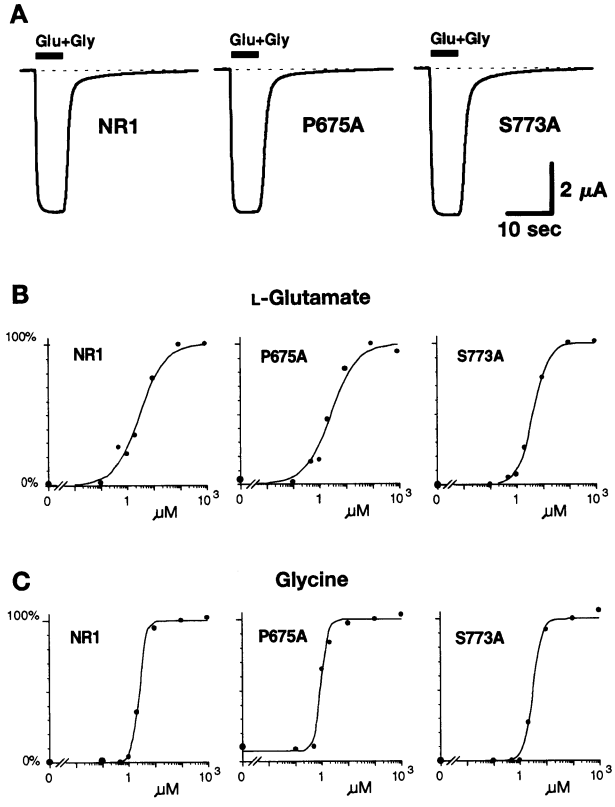

FIG. 4. Functional characterization of NMDA receptor glycosylation mutants. (*A*) All three constructs (NR1, P675A, and S773A) directed formation of functional NMDA receptors following expression in *Xenopus* oocytes. cRNA of NR1 and mutant constructs was prepared and coinjected (1:1) with ε1 cRNA (mouse NR2A clone, a generous gift of Masayoshi Mishina; ref. 39) into stage V or VI oocytes (75 nl each), as described (40). Whole oocyte currents elicited by agonist application (100 μM L-glutamate plus 100 μM glycine) at a holding potential of −50 mV are shown. (*B* and *C*) Dose–response curves for L-glutamate (in the presence of 100 μM glycine) and glycine (in the presence of 100 μM L-glutamate) were obtained by normalizing current responses to different concentration of agonist. Dose–response data were fitted with the Hill equation. The mutations had no significant effect on the EC_{50} values for glutamate (3–5 μM) or glycine (1–3 μM). Hill coefficients for L-glutamate (1.0–1.4) or glycine (2.6–3.5) were also unaffected.

seemed to have influenced the glycine binding site, since small (10%) current responses were obtained with mutant P675A in nominal glycine-free solutions (Fig. 4*C*). This region has previously been proposed to form part of the glycine binding site (29).

We have uncovered a previously unrecognized homology in pore regions across two families of ion channels, glutamate receptors and voltage-dependent K channels, suggesting that their pore structure is conserved. The glycosylation data presented here place both extremes of the M3–M4 linker extracellularly. Therefore, the first three putative transmembrane segments (M1–M3) together must cross the membrane an even number of times. This suggests a hairpin structure for M2, if we assume that M1 and M3 are α-helical transmembrane segments that cross the membrane once. A definitive test of this hypothesis will require an intracellular assignment of both linkers flanking M2.

Taken together, the amino acid homology and the glycosylation data support the hypothesis that ion conduction pathways in K channels and glutamate receptors are structurally conserved hairpin motifs. This topology further implicates a contribution by the M3–M4 linker to the ligand binding domain of glutamate receptors. Our model also provides further insight into the evolution of ion channels. K channels evolutionarily predate the Na and Ca channels with which they share a common ancestor. Ligand-gated channels are relatively new, arising from an unknown precursor (1). The extended homology in the pore regions of glutamate receptors and voltage-gated K channels suggests the possibility of a common origin for these ion channels. The parallel pore topology may also allow for renewed interpretation of structure–function results from two formerly unrelated families of channels.

This work was supported by a grant from the National Institute of Neurological Disorders and Stroke (NS31557 to A.M.J.V.D.).

M.W.W. was supported by National Institutes of Health predoctoral training grant GM07105.

1. Hille, B. (1992) *Ionic Channels of Excitable Membranes* (Sinauer, Sunderland, MA).
2. Neher, E. & Sakmann, B. (1983) *Single-Channel Recording* (Plenum, New York).
3. Raymond, L. A., Blackstone, C. D. & Huganir, R. L. (1993) *Nature (London)* **361,** 637–641.
4. Wooley, G. A. & Wallace, B. A. (1992) *J. Membr. Biol.* **129,** 109–136.
5. Li, M., Unwin, N., Stauffer, K. A., Jan, Y.-N. & Jan, L. Y. (1994) *Curr. Biol.* **4,** 110–115.
6. Unwin, N. (1993) *Cell* **72,** Suppl., 31–41.
7. Langosch, D., Thomas, L. & Betz, H. (1988) *Proc. Natl. Acad. Sci. USA* **85,** 7394–7398.
8. Nayeem, N., Green, T. P., Martin, I. L. & Barnard, E. A. (1994) *J. Neurochem.* **62,** 815–818.
9. Yellen, G., Jurman, M. E., Abramson, T. & Mackinnon, R. (1991) *Science* **251,** 939–942.
10. Hartmann, H. A., Kirsch, G. E., Drewe, J. A., Taglialatela, M., Joho, R. H. & Brown, A. M. (1991) *Science* **251,** 942–945.
11. Yool, A. J. & Schwarz, T. L. (1991) *Nature (London)* **349,** 700–704.
12. Heginbotham, L., Abramson, T. & Mackinnon, R. (1992) *Science* **258,** 1152–1155.

13. Bormann, J., Rundstrom, N., Betz, H. & Langosch, D. (1993) *EMBO J.* **12,** 3729–3737.
14. Noda, M., Takahashi, H., Tanabe, T., Toyosato, M., Kikyotani, S., Furutani, Y., Hirose, T., Takashima, H., Inayama, S., Miyata, T. & Numa, S. (1983) *Nature (London)* **302,** 528–532.
15. Mackinnon, R., Heginbotham, L. & Abramson, T. (1990) *Neuron* **5,** 767–771.
16. Goldstein, S. A., Pheasant, D. J. & Miller, C. (1994) *Neuron* **12,** 1377–1388.
17. Verdoorn, T. A., Burnashev, N., Monyer, H., Seeburg, P. H. & Sakmann, B. (1991) *Science* **252,** 1715–1718.
18. Burnashev, N., Schoepfer, R., Monyer, H., Ruppersberg, J. P., Gunther, W., Seeburg, P. & Sakmann, B. (1992) *Science* **257,** 1415–1419.
19. Bormann, J., Rundstrom, N., Betz, H. & Langosch, D. (1993) *EMBO J.* **12,** 3729–3737.
20. Imoto, K., Busch, C., Sakmann, B., Mishina, M., Konno, T., Nakai, J., Bujo, H., Mori, Y., Fukada, K. & Numa, S. (1988) *Nature (London)* **335,** 645–648.
21. Chavez, R. A. & Hall, Z. W. (1992) *J. Cell Biol.* **116,** 385–393.
22. Tingley, W. G., Roche, K. W., Thompson, A. K. & Huganir, R. L. (1993) *Nature (London)* **364,** 70–73.
23. Roche, K. W., Raymond, L. A., Blackstone, C. & Huganir, R. L. (1994) *J. Biol. Chem.* **269,** 11679–11682.
24. Taverna, F. A., Wang, L. Y., MacDonald, J. F. & Hampson, D. R. (1994) *J. Biol. Chem.* **269,** 14159–14164.
25. Guy, H. R. (1984) *Biophys. J.* **45,** 249–261.
26. Finer-Moore, J. & Stroud, R. M. (1984) *Proc. Natl. Acad. Sci. USA* **81,** 155–159.
27. Seeburg, P. H. (1993) *Trends Pharmacol. Sci.* **14,** 297–303.
28. O'Hara, P. J., Sheppard, P. O., Thogersen, H., Venezia, D., Haldeman, B. A., McCrane, V., Houamed, K. M., Thomsen, C., Gilbert, T. L. & Mulvihill, E. R. (1993) *Neuron* **11,** 41–52.
29. Kuryatov, A., Laube, B., Betz, H. & Kuhse, J. (1994) *Neuron* **12,** 1291–1300.
30. Wo, Z. G. & Oswald, R. E. (1994) *Proc. Natl. Acad. Sci. USA* **91,** 7154–7158.
31. Gafvelin, G. & Von Heijne, G. (1994) *Cell* **77,** 401–412.
32. Gonnet, G. H., Cohen, M. A. & Bennet, S. A. (1992) *Science* **256,** 1443–1445.
33. Melton, D. A. (1987) *Methods Enzymol.* **152,** 288–304.
34. Colman, A. (1900) in *Transcription and Translation: A Practical Approach*, eds. Hames, B. B. & Higgins, S. J. (IRL, Oxford), pp. 271–302.
35. Brose, N., Gasic, G. P., Vetter, D. E., Sullivan, J. M. & Heinemann, S. F. (1993) *J. Biol. Chem.* **268,** 22663–22671.
36. Sarkar, G. & Sommer, S. S. (1990) *BioTechniques* **8,** 404–407.
37. Lis, H. & Sharon, N. (1994) *Eur. J. Biochem.* **218,** 1–27.
38. Moriyoshi, K., Masu, M., Ishii, T., Shigemoto, R., Mizuno, N. & Nakanishi, S. (1991) *Nature (London)* **354,** 31–37.
39. Meguro, H., Mori, H., Araki, K., Kushiya, E., Kutsuwada, T., Yamazaki, M., Kumanishi, T., Arakawa, M., Sakimura, K. & Mishina, M. (1992) *Nature (London)* **357,** 70–74.
40. VanDongen, A. M. J., Frech, G. C., Drewe, J. A., Joho, R. H. & Brown, A. M. (1990) *Neuron* **5,** 433–443.